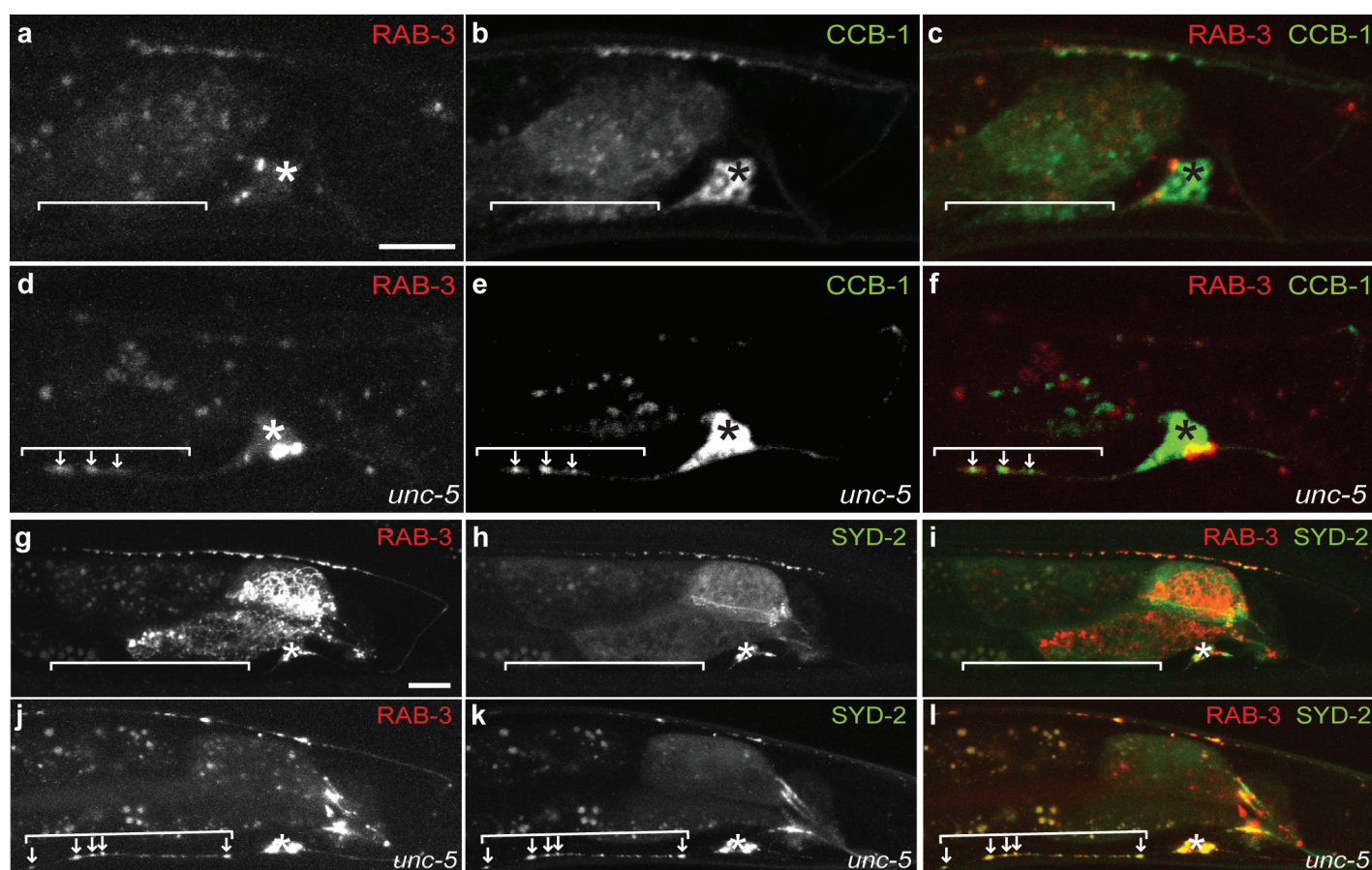
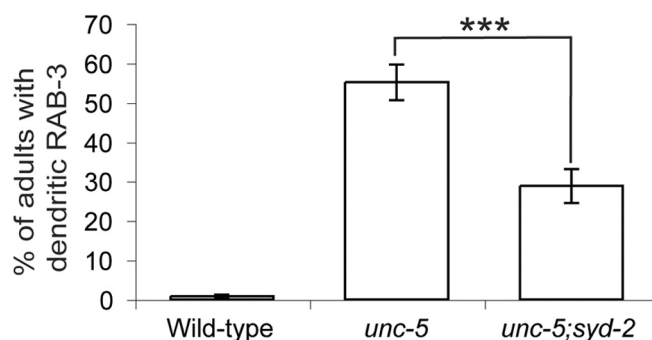


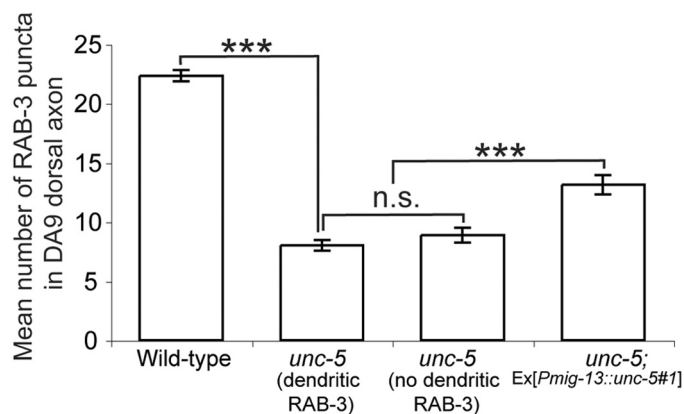
Supplementary Figure 1. Multiple synaptic vesicle proteins mislocalize to the dendrite in *unc-5* and *unc-6/netrin* mutants in the early larval stage. a-d, A representative wild-type L1 animal co-expressing CFP::RAB-3, SNB-1/synaptobrevin::YFP, and SNG-1/synaptogyrin::mCherry specifically in DA9 (*wyIs109*). Note that all three markers are absent in the DA9 dendrite. e-h, A representative *unc-5* mutant at the L1 stage (*wyIs109*) where all three synaptic vesicle markers colocalize (arrows) in the dendrite of DA9. The signal in the middle of the worm is gut autofluorescence. Anterior, left and dorsal, top. Brackets, dendrites. Asterisks, cell bodies. Scale bar, 10 μ m.



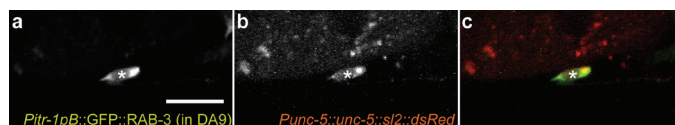
Supplementary Figure 2. A calcium channel subunit and an active zone protein mislocalize to the dendrite in *unc-5* and *unc-6/netrin* mutants. a-c, A representative wild-type L1 animal co-expressing the calcium channel β subunit GFP::CCB-1 and synaptic vesicle marker mCherry::RAB-3 specifically in DA9 (*wyEx771*). Note that both markers are absent in the DA9 dendrite. d-f, A representative *unc-5* mutant at the L1 stage with GFP::CCB-1 and mCherry::RAB-3 (*wyEx771*) present in the DA9 dendrite. g-i, A representative wild-type adult co-expressing the active zone marker GFP::SYD-2/ α -liprin and synaptic vesicle marker mCherry::RAB-3 specifically in DA9 (*wyEx2055*). Note that both markers are absent in the DA9 dendrite. j-l, A representative *unc-5* mutant adult with GFP::SYD-2/ α -liprin and mCherry::RAB-3 (*wyEx2055*) present in the DA9 dendrite. Arrows indicate colocalization of the markers. The signal in the middle of the worm is gut autofluorescence. Anterior, left and dorsal, top. Brackets, dendrites. Asterisks, cell bodies. Scale bar, 10 μ m.



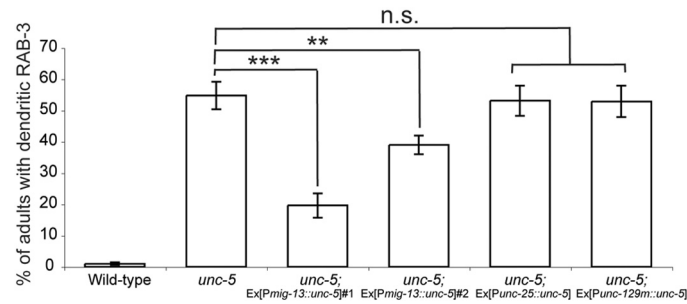
Supplementary Figure 3. The mislocalization defect in *unc-5* mutants is partially dependent on the function of SYD-2/ α -liprin. Penetrance of the mislocalization defect in animals expressing GFP::RAB-3 specifically in DA9 (*wyIs85*). Error bars, standard error of proportion. $n > 100$. ***, $p < 0.0001$, chi squared test.



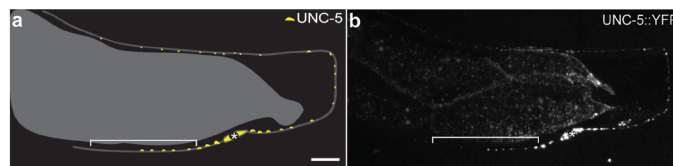
Supplementary Figure 4. The mislocalization of presynaptic components to the DA9 dendrite does not correlate with presynaptic patterning defects in the dorsal axon of *unc-5* mutants. The average number of GFP::RAB-3 puncta (*wyIs85*) in the DA9 dorsal axon in wild-type and *unc-5* mutant adults with or without dendritic GFP::RAB-3. Error bars, standard error. $n = 40$. ***, $p < 0.0001$, t test. n.s., not significant.



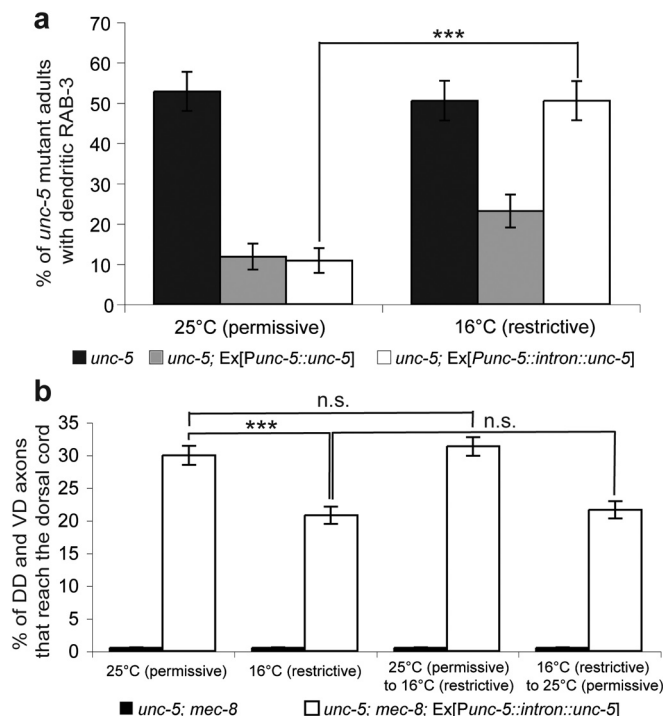
Supplementary Figure 5. UNC-5 is endogenously expressed in DA9. a-c, A representative *unc-5; lin-18/ryk* mutant adult expressing both RAB-3 specifically in DA9 (a, *wyIs85*) and cytoplasmic dsRed driven by an endogenous *unc-5* promoter (b, *wyEx1498*). Note the colocalization of both markers in the DA9 cell body (asterisk). This transgenic line is mosaic and the animal shown expresses dsRed in DA9 but not in nearby cells that express UNC-5 endogenously. The mutation in LIN-18/Ryk does not affect the expression pattern of UNC-5. Scale bar, 10 μ m.



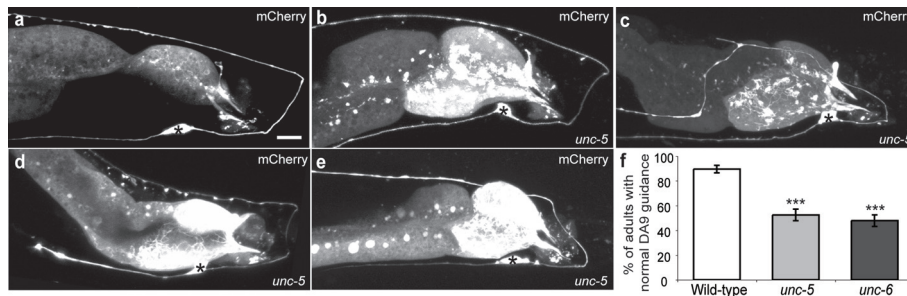
Supplementary Figure 6. UNC-5 acts cell-autonomously in DA9 to exclude GFP::RAB-3 from the DA9 dendrite. Expression of UNC-5 in the VD/DD neurons (Ex[Punc-25::unc-5]) or the dorsal body wall muscles (Ex[Punc-129m::unc-5]) does not rescue the mislocalization defect in *unc-5* mutant adults expressing GFP::RAB-3 specifically in DA9 (*wyIs85*). $n > 100$. ***, $p < 0.0001$; **, $p < 0.005$; chi squared test. n.s., not significant.



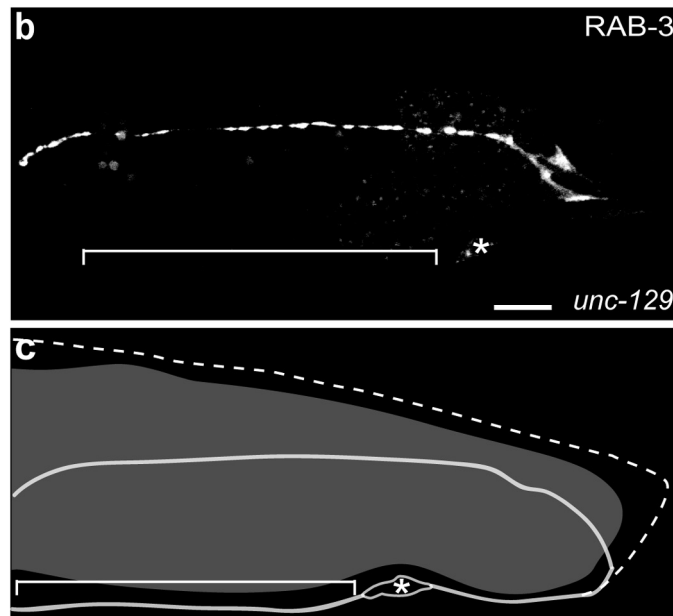
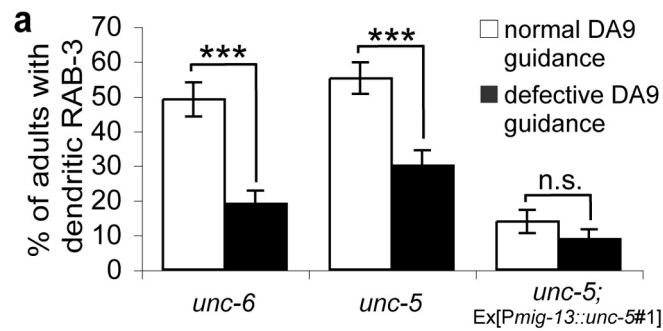
Supplementary Figure 7. UNC-5 is enriched in the dendrite and ventral axon. a, b, A diagram and micrograph of a representative wild-type adult expressing UNC-5::YFP specifically in DA9 (*wyEx1277*). The signal in the middle of the worm is gut autofluorescence. Anterior, left and dorsal, top. Brackets, dendrites. Asterisks, cell bodies. Scale bar, 10 μ m.



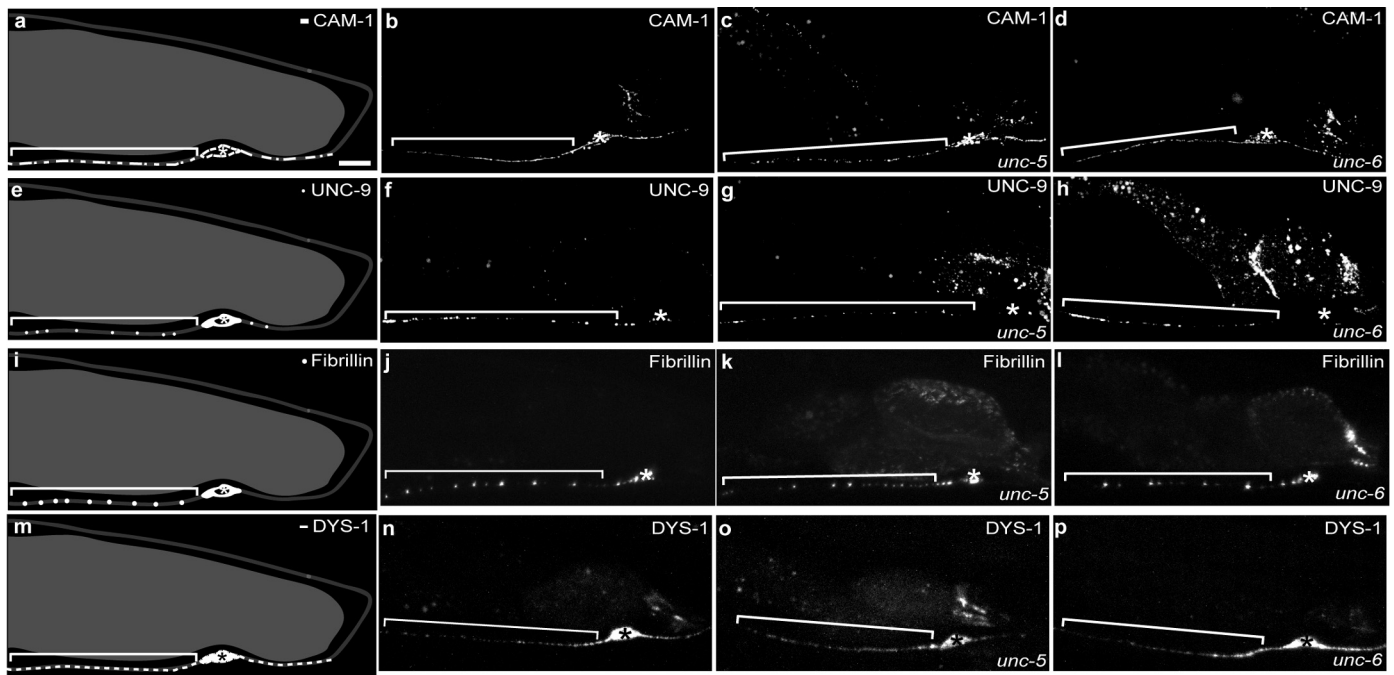
Supplementary Figure 8. Temperature-dependent regulation of UNC-5. a, Insertion of *mec-2* intron 9 results in the loss of *unc-5* function at 16°C. Penetrance of dendritic RAB-3 in *unc-5*, *unc-5*; Ex[Punc-5::unc-5] (*wyEx1228*), and *unc-5*; Ex[Punc-5::intron::unc-5] (*wyEx2308*) mutant adult animals expressing GFP::RAB-3 specifically in DA9. Error bars, standard error of proportion. $n > 100$ mutant animals. ***, $p < 0.0001$, chi squared test. b, Expression of UNC-5 (Ex[Punc-5::intron::unc-5], *wyEx2306*) is sufficient to partially rescue VD and DD axon guidance defects in *unc-5*; *mec-8* mutants. The rescuing activity of this construct is significantly stronger at 25°C versus 16°C. The mutants express a cytoplasmic marker in the VD and DD neurons (Ex[Punc-47l::rfp], *wyIs75*). Temperature shifts were conducted in animals at the L3 and early L4 larval stages and phenotypes were scored in gravid adults. The effects observed are less dramatic than in Fig. 2E due to the mosaic nature of the *unc-5* promoter, which drives expression more consistently in DA9 than in all of the DD and VD neurons. Error bars, standard error of proportion. $n > 950$ axons. ***, $p < 0.0001$, chi squared test. n.s., not significant.



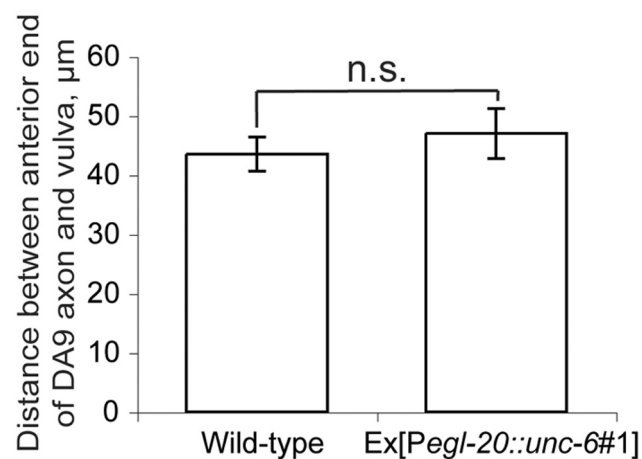
Supplementary Figure 9. DA9 guidance is unaffected in a significant portion of *unc-5* and *unc-6*/*netrin* mutants. a, b, Representative wild-type (a) and *unc-5* mutant (b) adults expressing a DA9-specific cytoplasmic marker (*wyEx1902*) that exhibit normal DA9 guidance. c–e, *unc-5* mutant adults with varying degrees of DA9 guidance defects. The signal in the middle of the worm is gut autofluorescence. Anterior, left and dorsal, top. Asterisks, cell bodies. Scale bar, 10 μ m. f, Penetrance of normal DA9 guidance in wild-type, *unc-5* and *unc-6*/*netrin* mutant adults expressing a cytoplasmic marker specifically in DA9. Error bars, standard error of proportion. n > 100. ***, p < 0.0001 compared to wild-type animals, chi squared test.



Supplementary Figure 10. DA9 guidance defects do not cause mislocalization of GFP::RAB-3 to the dendrite. a, Penetrance of the mislocalization defect in *unc-5* and *unc-6*/*netrin* mutant adults co-expressing both GFP::RAB-3 and a cytoplasmic marker specifically in DA9 (*wyIs85*; *wyEx1902*). Error bars, standard error of proportion. n > 100. ***, p < 0.0001, chi squared test. n.s., not significant. b, A representative *unc-129*/*Tgfb* mutant adult with DA9 guidance defects but no GFP::RAB-3 (*wyIs85*) in the dendrite. The signal in the middle of the worm is gut autofluorescence. Scale bar, 10 μ m. c, A diagram of defective DA9 axon guidance in the *unc-129*/*Tgfb* mutant adult shown in b. The dotted line depicts normal DA9 axon guidance. Anterior, left and dorsal, top. Asterisks, cell bodies.



Supplementary Figure 11. Four dendritic proteins are localized properly in *unc-5* and *unc-6/netrin* mutants. a, e, i, m, Diagrams of CAM-1/Ror tyrosine kinase, UNC-9/innexin, Fibrillin, or DYS-1/dystrophin localization in DA9. Note the absence of these proteins from the commissure and dorsal axon. b, f, j, n, Representative wild-type adults expressing either CAM-1::YFP (b, *wyEx403*), UNC-9::YFP (f, *wyEx1054*), Fibrillin::YFP (j, *wyEx2396*), or DYS-1::YFP (n, *wyEx2430*) specifically in DA9. c, d, g, h, j, k, l, o, p, The localization of all four dendritic proteins is unaltered in *unc-5* and *unc-6/netrin* mutant adults. The signal in the middle of the worm is gut autofluorescence. Anterior, left and dorsal, top. Asterisks, cell bodies. Scale bar, 10 μ m.



Supplementary Figure 12. The ectopic expression of UNC-6/netrin does not alter the dorsal axon length of DA9. Dorsal axon length of DA9 as measured from the anterior end of the axon to the vulva, a landmark for the mid-body. Animals in the mid-L4 larval stage expressing a cytoplasmic marker specific to DA9 (*wyEx1902*) with or without the *egl-20::unc-6/netrin* transgene (*wyEx1904*) were imaged and the axon length relative to the vulva was measured. Error bars, standard error. n = 30. n.s., not significant. t test.